



Published in final edited form as:

New Phytol. 2023 November ; 240(3): 1082–1096. doi:10.1111/nph.19219.

An interplay between bZIP16, bZIP68 and GBF1 regulates nuclear photosynthetic genes during photomorphogenesis in Arabidopsis

Louise Norén Lindbäck^{1,*}, Yan Ji², Luis Cervela-Cardona², Xu Jin², Ullas V. Pedmale³, Åsa Strand²

¹Umeå Plant Science Centre, Department of Forest Genetics and Plant Physiology, Swedish University of Agricultural Sciences, SE-901 83 Umeå, Sweden;

²Umeå Plant Science Centre, Department of Plant Physiology, Umeå University, SE-901 87 Umeå, Sweden.

³Cold Spring Harbor Laboratory, Cold Spring Harbor, New York 11724, USA.

Summary

The development of a seedling into a photosynthetically active plant is a crucial process. Despite its importance, we do not fully understand the regulatory mechanisms behind the establishment of functional chloroplasts.

We herein provide new insight into the early light response by identifying the function of three basic region/leucine zipper (bZIP) transcription factors; bZIP16, bZIP68 and GBF1. These proteins are involved in the regulation of key components required for the establishment of photosynthetically active chloroplasts. The activity of these bZIPs is dependent on the redox status of a conserved cysteine residue which provides a mechanism to finetune light-responsive gene expression.

The blue light cryptochrome (CRY) photoreceptors provide one of the major light-signaling pathways, and bZIP target genes overlap with one third of CRY-regulated genes with an enrichment for photosynthesis/chloroplast associated genes. bZIP16, bZIP68 and GBF1 were demonstrated as novel interaction partners of CRY1. The interaction between CRY1 and bZIP16 was stimulated by blue light. Furthermore, we demonstrate a genetic link between the bZIP proteins and cryptochromes as the *cry1cry2* mutant is epistatic to the *cry1cry2bzip16bzip68gbf1* mutant.

bZIP16, bZIP68 and GBF1 regulate a subset of photosynthesis associated genes in response to blue light critical for a proper greening process in Arabidopsis.

*Corresponding author. **Contact:** lindbacklouise@gmail.com.

Author Contributions: LNL, YJ and ÅS planned and designed the research. LNL, YJ, LCC and XJ performed the research with the following exception: UVP performed cloning of the Flag-CRY1 construct and provided this material. LNL wrote the manuscript, all authors reviewed and commented on the manuscript.

Competing interests:
None declared.

Keywords

bZIP; chloroplast development; cryptochrome; light signaling; photomorphogenesis; *Arabidopsis thaliana*

Introduction

A germinating seed buried under soil displays skotomorphogenic growth characterized by fast growing hypocotyls, closed cotyledons and a protective apical hook until light is reached. Upon exposure to light, the seedling initiates photomorphogenic development by hypocotyl elongation inhibition, cotyledon expansion and development of functional chloroplasts in order to start performing photosynthesis. Extensive transcriptional reprogramming drives the morphological changes necessary to establish a green photosynthetically active seedling, which includes the establishment of mature chloroplasts. In dark-germinated seedlings, plastids present as either undifferentiated proplastids or the dark-grown intermediate etioplast will develop into photosynthetically active chloroplasts (Pogson & Albrecht, 2011). As the plastid has retained its own genome, which is remnant from their genome as free-living bacteria, the establishment of functional chloroplasts is a complex process involving both nuclear and plastid gene expression. To coordinate their activities, there must be a close interaction between the nucleus and the plastids through anterograde and retrograde signaling pathways. The initial light signal perceived by a dark grown seedling triggers the activation of photoreceptors. Plants can detect almost all wavelengths of light using three major classes of photoreceptors: the red/far-red absorbing phytochromes (PHYs), the blue light/UV-A absorbing cryptochromes (CRYs), phototropins (PHOTs) and ZTL-type photoreceptors, and the UV-B absorbing UVR8 photoreceptor (Galvao & Fankhauser, 2015). Photoreceptors can sense the intensity, direction, duration, and wavelength of light and initiate intracellular signaling pathways in response to light. These pathways involve proteolytic degradation of signaling components and large reorganization of the transcriptional program to modulate the growth and development of plants (Chen et al., 2004). When dark grown seedlings are exposed to light as much as one-third of the nuclear encoded genes show transcriptional changes and among the genes most dramatically up-regulated in the light are genes encoding chloroplast-targeted proteins (Ma et al., 2001). These photosynthesis associated nuclear genes (*PhANGs*) include genes such as subunits of photosystem II (PSII), photosystem I (PSI) and the carbon fixation reactions of the Calvin-Benson cycle (Allen et al., 2011).

The G-box *cis*-element has been shown to be enriched in the promoters of genes responding to different light signals (Kleine et al., 2007) and both the basic region/leucine zipper (bZIP) and basic helix-loop-helix (bHLH) transcription factors are known to interact with this element (Siberil et al., 2001). bZIPs are known to also bind other *cis*-elements, especially with an ACGT core, whereas bHLHs rather bind to the CANNTG consensus sequence (Siberil et al., 2001; Jakoby et al., 2002). There are 75 members of the bZIP family in *Arabidopsis* and these transcription factors are involved in the regulation of a variety of processes such as light and stress signaling, hormone signaling, plant development and pathogen defense (Siberil et al., 2001; Jakoby et al., 2002; Llorca et al.,

2014). The Arabidopsis bZIP proteins have been clustered into 10 subgroups (A-I and S) according to their sequence similarities of the basic region, size of the leucine zipper and presence of other common domains (Jakoby et al., 2002). The bZIP protein ELONGATED HYPOCOTYL5 (HY5) and its homolog HYH are known to bind the G-box element and are grouped together in the H-group (Lee et al., 2007). Three members of the G-group transcription factors, bZIP16, bZIP68 and G-box-binding factor 1 (GBF1), have been identified as G-box binding proteins and were shown to respond to redox changes (Shaikhali et al., 2012). Out of these proteins, GBF1 has been most studied and was initially identified as a G-box binding protein (Schindler et al., 1992). GBF1 has been described to regulate blue light-mediated photomorphogenic growth and to interact with CONSTITUTIVE PHOTOMORPHOGENIC1 (COP1) and the bHLH transcription factor MYC2 which is a regulator of photomorphogenesis in blue light (Mallappa et al., 2006; Mallappa et al., 2008; Maurya et al., 2015). In addition to regulating light-mediated seedling development, GBF1 has been shown to inhibit CATALASE 2 (CAT2) expression during senescence and positively regulate PHYTOALEXIN DEFICIENT 4 (PAD4) to promote pathogen defense (Smykowski et al., 2015; Giri et al., 2017). bZIP16 has been described to be involved in the integration of light and hormone signaling pathways during early seedling development, and transcriptome analysis has shown that bZIP16 primarily functions as a repressor regulating light-, gibberellic acid (GA)-, and abscisic acid (ABA)-responsive genes (Hsieh et al., 2012). bZIP68 was shown to be involved in sensing oxidative stress and mediate transcriptional reprogramming to balance stress tolerance and plant growth (Li et al., 2019). In this report, we present findings suggesting that these three bZIP proteins together play a role in the regulation of key components required for the establishment of photomorphogenic growth triggered by cryptochrome mediated light response in Arabidopsis.

Materials and Methods

Plant Material and Growth Conditions.

Arabidopsis thaliana (L.) Heynh. seeds were plated on 1 x MS plates and vernalized for 2 days at 4 °C in darkness. The plates were exposed to 100 µmol/m/s white light, 22 °C, for 4 h to induce germination and subsequently kept in darkness for 5 days. The etiolated seedlings were thereafter exposed to 100 µmol/m/s LED white light (Fig. S1), 20 µmol/m/s LED blue light, or 20 µmol/m/s LED red light and analysed at the indicated time points. All *bzip* mutants were in the Columbia background, *bzip16* (Salk_095123), *bzip68* (Salk_147015) and *gbf1* (Salk_144534) and used to generate the *bzip* triple mutant. Seeds for the T-DNA insertion lines were obtained from NASC stock centre. The *crybzip* quintuple mutant was generated by crossing the *bzip* triple mutant to a *cry1cry2* double mutant (*cry1-304*, *cry2-1*). The construction of 35S::bZIP16WT and 35S::bZIP16C1 binary vectors were described previously (Shaikhali et al., 2012). The 35S::bZIP16C2 binary vector was generated by amplifying the full length coding sequence of bZIP16C2 from the pET100D TOPO vector (Shaikhali et al., 2012). The obtained sequence was subsequently cloned into pDONR207 entry vector and pH2GW7.0 binary vector using the Gateway system (Invitrogen). Transgenic lines in the *bzip* triple mutant background were generated by floral dip method using *Agrobacterium tumefaciens* strain GV3101 (Clough & Bent, 1998).

Cotyledon opening measurements.

5 days old etiolated seedlings were transferred to 100 $\mu\text{mol}/\text{m}^2/\text{s}$ constant white light and scanned at the indicated time points. At least 25 seedlings were measured for the wild type Col, *bzip* triple, *cry1cry2*, and *crybzip* quintuple mutant and at least 40 seedlings were measured for the *35S::bZIP16WT/C1/C2* transgenic lines. The measurement of the opening angle was performed with ImageJ software (Schindelin et al., 2012).

Chlorophyll measurements.

For chlorophyll content analysis, 5 days old etiolated seedlings were transferred to 100 $\mu\text{mol}/\text{m}^2/\text{s}$ constant white light for 12, 24, 48 and 96 h. Samples were ground with liquid nitrogen and 1 mL of buffered acetone (80% acetone, 25 mM HEPES pH 7.5) was added to 100 mg of material and incubated over night at 4 °C. Chlorophyll content was determined as previously described (Porra et al., 1989).

Transmission Electron Microscopy.

The chloroplast development was analysed in 5 days old etiolated seedlings exposed to 100 $\mu\text{mol}/\text{m}^2/\text{s}$ constant white light for 24 h. The sample preparation and transmission electron microscopy were performed as described previously (Dubreuil et al., 2018). In short, the samples were fixed using 2.5% (v/v) glutaraldehyde in 0.1 M cacodylate buffer overnight at 4°C and thereafter washed three times in 0.1 M cacodylate buffer. Postfixation was performed with 1% (v/v) osmium tetroxide in the medium buffer for 1 h followed by two washes in distilled water. Samples were dehydrated with 50%, 70%, 95%, and 100% ethanol, infiltrated and embedded in Spurr's resin. Using a Diatome diamond knife on a Leica EM UC7 device, thin sections (60–90 nm) were collected onto copper grids and treated with 5% uranyl acetate in water for 20 min. Sato's lead staining was performed for 5 min. Sections were examined in a JEOL 1230 transmission electron microscope, and digital images were captured using a Gatan MSC 600CW camera.

RNA Isolation, cDNA Synthesis, and Real-Time PCR.

Total RNA was isolated using the EZNA Plant RNA mini kit and DNase treatment was performed using Thermo Scientific DNase I, RNase-free according to the manufacturer's instructions. Using the iScript cDNA Synthesis Kit (Bio-Rad) cDNA was synthesized from 0.5 μg of total RNA according to the manufacturer's instructions. cDNA was diluted 10-fold and 3 μL of the diluted cDNA was used in a 10 μL iQ SYBR Green Supermix reaction (Bio-Rad). All reactions were performed in two technical replicates using primers as indicated (Table S1). qRT PCR was run in CFX96 Real time system (Bio-Rad) and monitored by using the CFX Manager (Bio-Rad). The adjustment of baseline and threshold was done according to the manufacturer's recommendations. Data were analysed by using LinRegPCR (Pfaffl, 2001; Ramakers et al., 2003) and the relative abundance of all transcripts amplified was normalized to the constitutive expression level of UBI or PP2A.

Analyses of DAP-/RNA-seq. data.

The DAP-seq data for bZIP16 and bZIP68 were downloaded at <http://neomorph.salk.edu/PlantCistromeDB> (O'Malley et al., 2016). The accession number for the raw and processed

data of DAP-seq. has been uploaded to GEO: GSE60143. CRY-regulated genes were the genes with differential expression in both blue light-grown WT/dark-grown WT and blue light-grown WT/blue light-grown *cry1cry2*, concluded from RNA-seq analyses (He et al., 2015). The RNA-seq. data has the accession number GSE58552. The GO enrichment analysis was performed in the gene ontology resource (<http://geneontology.org/>) and only the results for FDR $P < 0.05$ are shown.

Co-immunoprecipitation.

The bZIP16, bZIP68 and GBF1 coding sequences were amplified from WT cDNA and cloned into pDONR221 using Gateway BP Clonase II (Invitrogen). The pDONR221-bZIP16, pDONR221-bZIP68 and pDONR221-GBF1 were recombined with pDONRP4-P1R-UBQ10promoter and pDONRP2R-P3-9xMyc entry clones in pK7m34GW expression vector using MSLR (MultiSite LR Gateway, Invitrogen). The CRY1 coding sequence was amplified from WT cDNA and cloned into pDONRP2R-P3 using Gateway BP Clonase II (Invitrogen). pDONRP2R-P3-CRY1 was recombined together with pDONRP4-P1R-UBQ10promoter and pDONR221-2xStrepII-6xHis-3xFlag entry clones in pB7m34GW expression vector using MSLR technology (MultiSite LR Gateway, Invitrogen). The final expression vectors *UBQ10pro::bZIP16-Myc* (or *UBQ10pro::bZIP68-Myc*, *UBQ10pro::GBF1-Myc*) and *UBQ10pro::Flag-CRY1* were transformed into *Agrobacterium tumefaciens* and transiently expressed in the described combinations into *Nicotiana benthamiana* (*Nicotiana tabacum* L.) leaves by agroinfiltration. Leaves were sampled 3 days post infiltration. Immunoprecipitation was performed using ground tissue resuspended in SII buffer (100 mM sodium phosphate pH 8.0, 150 mM NaCl, 5 mM EDTA, 5 mM EGTA, 0.1% Triton X-100, 10 mM NaF, 1.5x protease inhibitor cocktail and 75 μ M MG132). The extracts were sonicated at 30% 0.5 s on/off for a total of 10 s and clarified by 2x high speed centrifugation for 10 min. 2 mg total protein was used for each sample and incubated with anti-c-Myc magnetic beads (Pierce) for 1 h rotating at 4 °C. The beads were washed 3x with 800 μ l SII buffer and thereafter eluted in 2x Laemmli sample buffer. The eluate was used for Western blot analysis with anti-Flag-HRP (Sigma) for detection of Flag-CRY1 and anti-Myc (ab32, abcam) for detection of bZIP16-Myc, bZIP68-Myc and GBF1-Myc.

Protoplast Split-LUC Assay.

Protoplasts were isolated protocol described in Yoo et al., 2007 with slight modifications. Briefly, approximately 20 leaves (1.5 cm length) were chopped using a clean razor blade and subsequently digested in 20 mL of enzyme solution for 2 hours with gentle shaking. After digestion, the mixture was filtered, and the protoplasts were pelleted by centrifugation at 100 g for 3 minutes. The pellet was subsequently washed and centrifuged again at 100 g for 1 minute. Following this step, supernatant was removed, and protoplasts were resuspended in 5 mL MMG solution, yielding an approximate working concentration of 2×10^5 cells per mL. For DNA transfection and luminescence measurement, the assay was performed using a modified version of Chen et al., 2008. Succinctly, CRY1 or bZIP16 coding sequences were cloned to be expressed under a 35S promoter and fused to either the NLuc or CLuc part of the Luciferase sequence (Yu et al., 2020). In a 96-well plate, 50 μ L protoplasts were mixed with 5 μ g of each desired vectors in four replicates. PEG solution was added, and transfection occurred for 15 min, followed by W5 solution termination. Protoplasts were

allowed to settle, and supernatant was replaced with WI solution containing D-luciferin. After overnight incubation at 22°C, luminescence was recorded using a GloMax[®] Navigator microplate reader with a 2-second integration time. For investigation of the BL stimulation of the interaction, the constructs were transiently expressed in the described combinations into *Nicotiana benthamiana* leaves by agroinfiltration. Leaves were sampled 3 days post infiltration. Western blot analysis of controls for expression of the LUC fusion proteins was performed with an anti-Luciferase antibody produced in rabbit (L0159, Merck).

Statistical analyses.

The statistical significance of the results was analysed using Student t-test.

Results

bZIP16, bZIP68 and GBF1 are involved in the de-etiolation process and development of mature chloroplasts.

Previous studies have implicated that GBF1 and bZIP16 play a role during photomorphogenesis and that they, and bZIP68, are involved in the regulation of light-responsive genes (Mallappa et al., 2006; Hsieh et al., 2012; Shaikhali et al., 2012). We wanted to examine whether these bZIP proteins have a function during the de-etiolation process. bZIP16, bZIP68 and GBF1 belong to the G-group of bZIP transcription factors and bZIP16 shares 78% overall protein sequence similarity with bZIP68, 48% with GBF1 but less than 40% with GBF2–3 (Shaikhali et al., 2012). Considering the high similarity between bZIP16, bZIP68 and GBF1, and the fact that no visual phenotype was observed in the single mutants, redundancy between the different proteins could be an issue. Thus, we generated a *bzip* triple mutant by crossing the T-DNA insertion lines *bzip16* (Salk_095123), *bzip68* (Salk_147015) and *gbf1* (Salk_144534). The *bzip68* and *gbf1* T-DNA insertion lines are described previously (Shaikhali et al., 2012). No complete null allele could be identified for *bZIP16*, instead a knock-down *bzip16* line with significant down regulation of *bZIP16* transcript was used (Fig. S2a).

During the de-etiolation process, light inhibits hypocotyl elongation, initiates cotyledon opening and promotes the development of functional chloroplasts. In order to investigate whether the bZIP proteins are involved in the establishment of photomorphogenic growth, we monitored and analyzed 5 days old etiolated seedlings of wild type and the *bzip* triple mutant exposed to continuous white light (100 m⁻²s⁻¹). The seedlings were scanned in the dark and following exposure to light for a time series up to 24 h and analyzed for the cotyledon opening. We found that the cotyledon opening was delayed in the *bzip* triple mutant during the early time points and significantly different at 6 h compared to the wild type (Fig. 1a, b). Following 9 h, and particularly 12 and 24 h, the cotyledon opening of the *bzip* triple mutant seedlings reached the same degree as observed in wild type seedlings (Fig. 1a, b).

During early light response, the nuclear transcriptome undergoes major changes to promote chloroplast development and the accumulation of chlorophyll in order to establish photosynthetic activity. The seedlings of wild type and *bzip* triple mutant were photographed

in dark and following exposure to light during 96 h. In dark, the characteristic phenotype of etiolated seedlings was observed for both wild type and the *bzip* triple mutant; elongated hypocotyls and pale closed cotyledons (Fig. S3). Following 12 h of light exposure, the wild type seedlings showed increased greening until 96 h of exposure to light. In comparison to wild type seedlings, the *bzip* triple mutant displayed a pale phenotype during 12, 24 and 48 h of light exposure, while following 96 h of light the color of the *bzip* triple seedlings were like wild type (Fig. S3). The pale phenotype of the *bzip* triple mutant indicates that the chloroplast development and chlorophyll accumulation might be affected. Therefore, we analyzed the chlorophyll content in wild type and *bzip* triple mutant following transition to light. Wild type seedlings showed a significant accumulation of chlorophyll a and b after 12 h in the light and thereafter increasing levels of chlorophyll content until 96 h (Fig. 1c). In contrast, the *bzip* triple mutant displayed deficient accumulation of chlorophyll a and b compared to wild type following 12, 24, and 48 h of light exposure, but reached wild type levels after 96 h of light, consistent with the observed pale phenotype (Fig. 1c, S3).

To further investigate if the bZIP16, bZIP68, and GBF1 proteins play a role during early chloroplast development, we analyzed the chloroplast morphology following 24 h exposure to light by transmission electron microscopy (TEM). In wild type, the chloroplasts are fully developed with internal thylakoid membranes and grana stacks following 24 h of light exposure (Fig. 1d, e). The analysis of chloroplasts in the *bzip* triple mutant showed that the basic internal thylakoid membranes are formed, but that they lack grana structures, demonstrating that the chloroplast development is significantly delayed compared to wild type (Fig. 1f, g). In contrast to the *bzip* triple mutant, the *bzip16*, *bzip68* and *gbf1* single mutants did not display any obvious de-etiolation phenotype following the dark to light transition (Fig. S2b), indicating possible redundant functions of these bZIP proteins during the growth conditions used in this study. Taken together, these results demonstrate that the de-etiolation process is delayed in the *bzip* triple mutant compared to wild type.

The bZIP proteins regulate photosynthesis-related nuclear genes in response to light.

The bZIP16, bZIP68, and GBF1 transcription factors have been shown to regulate light-responsive genes such as the light-harvesting chlorophyll a/b-binding protein 2.4 (*LHCB2.4*) (Shaikhali et al., 2012). To further investigate which genes are specifically regulated by these bZIP proteins, we retrieved publicly available DAP-sequencing data sets, one each for bZIP16 and bZIP68 (O'Malley et al., 2016). DAP-sequencing is an *in vitro* high-throughput TF-DNA-binding assay which identifies genome wide TF binding targets (Bartlett et al., 2017). These two data sets were used for our analysis, and we found 1630 genes targeted by bZIP16 and 6979 genes targeted by bZIP68 with 1613 overlapping genes (Fig. 2a, Table S2). We further performed GO (gene ontology) term enrichment analysis using the 1613 common targets and identified terms with significant enrichment (false discovery rate; FDR<0.05). For the biological process, the top GO terms included the regulation of RNA biosynthesis, transcription and gene expression, and several terms related to photosynthesis and responses to light-related processes (Fig. 2a). The analysis of cellular component terms among the overlapping genes evidently demonstrates that the majority of the common bZIP16 and bZIP68 regulated genes are associated with the chloroplast and photosynthesis (Fig. 2a, Table S2).

To confirm that the observed phenotype of the *bzip* triple mutant is caused by misregulation of nuclear gene expression during de-etiolation, we analyzed the expression of selected genes found in the analyzed DAP-sequencing data. *LHCB1.1* and *LHCB2.4* are subunits of the Photosystem II antenna system, tightly regulated by light, and their promoters contain multiple G-box *cis*-elements (CACGTG) and/or the G-box core element (ACGT). As potential targets of the GBF1, bZIP16 and bZIP68 transcription factors, we analyzed the expression of the nuclear encoded *LHCB1.1* and *LHCB2.4* genes during the first 96 h following transition from dark to light in wild type and the *bzip* triple mutant. Following transition to light, *LHCB1.1* and *LHCB2.4* expression was strongly induced in wild type after 12 h of light exposure, and continuously increased until 96 h of light (Fig. 2b, c). Expression of *LHCB1.1* and *LHCB2.4* in the *bzip* triple mutant was also induced following 12 h of light but was significantly suppressed compared to wild type. *LHCB1.1* expression in the *bzip* triple mutant was similar to wild type in dark, thereafter significantly lower compared to wild type during the first 24 h of light and after 48 h *LHCB1.1* expression reached wild type levels (Fig. 2b). The *bzip* triple mutant showed down regulated levels of *LHCB2.4* already in the dark and significantly lower levels of expression during the first 96 h of light exposure (Fig. 2c).

Genes encoding the sigma factors were also found in the bZIP16 and/or bZIP68 DAP-sequencing data and given the phenotype those genes are interesting as potential targets of the bZIP transcription factors. Genes in the chloroplast genome are transcribed by two types of RNA polymerases; the nuclear encoded plastid RNA polymerase (NEP) (Hedtke et al., 1997) and the plastid encoded RNA polymerase (PEP) (Hu & Bogorad, 1990). PEP requires the nuclear-encoded sigma factors for both promoter recognition and DNA binding. Thus, these proteins determine which genes can be transcribed by PEP and provides nuclear control over the plastid gene expression (Hanaoka et al., 2003; Jarvis & Lopez-Juez, 2013). There are six sigma factors (SIG1 to SIG6) (Chi et al., 2015) and we analyzed the expression of *SIG1–6* in wild type and the *bzip* triple mutant following 24 h of light exposure, the time point where a strong down regulation of *LHCB1.1* and *LHCB2.4* was observed. *SIG1* and *SIG5* expression was significantly down regulated in the *bzip* triple mutant compared to wild type, while *SIG2, 3, 4* and *6* expression was like wild type (Fig. 2d; S4a–f). Previous analysis of the light induction profiles of *SIG1–6* expression has shown that *SIG1* is induced by red and blue light whereas *SIG5* is induced by blue light alone (Onda et al., 2008). This induction is also dependent on the fluence intensity and *SIG1* expression was demonstrated to increase to a plateau under low-fluence blue light while *SIG5* expression was similar to *SIG1* under low-fluence blue light but further enhanced with increased fluence rate, which was not observed for *SIG1* (Onda et al., 2008). The induction profiles following exposure to light for 12 and 24 h in the light condition used for our studies demonstrates that the expression of *SIG5* was most strongly induced, followed by *SIG1* while *SIG2, 3, 4* and *6* showed weaker expression profiles (Fig. S4a–f). The stronger induction of *SIG1* and *SIG5* compared to the other *SIGs* could possibly explain why only those genes are affected in the *bzip* triple mutant, thus it cannot be ruled out that the bZIP proteins may regulate additional *SIGs* under other light conditions considering both wavelength and intensity. In addition to the *SIG* and *LHCB* genes, a large number of bZIP16/68 nuclear target genes linked to light responses were identified in the DAP-seq analyses (Fig. 2a, Table S2).

To further demonstrate the importance of the bZIP proteins during de-etiolation and plastid processes, we analyzed the expression of four selected genes (Fig. S5). *PSB29/THF1* encodes a photosystem II reaction center protein (PSB29) also called Thylakoid formation 1 (THF1) which is involved in vesicle-mediated formation of thylakoid membranes. Expression is induced in response to light and *thf1* antisense lines have abnormal chloroplasts with loosely stacked thylakoid membranes early in leaf development (Wang et al., 2004). The plastid transcription factor TCP13 is a trans-acting factor of the *psbD* light-responsive promoter involved in the control of leaf differentiation (Hur et al., 2019). The RelA/SpoT homolog RSH3 protein is involved in guanosine tetraphosphate synthesis which can repress chloroplast gene expression and reduce chloroplast size (Romand et al., 2022). The *GATA transcription factor 2 (GATA2)* encodes a zinc finger transcription factor known to be a positive regulator of photomorphogenesis (Luo et al., 2010). All of these four genes were found to be down regulated in the *bzip* triple mutant following exposure to 24 h of light, further linking the observed phenotypes of the *bzip* triple mutant to the regulation of nuclear gene expression in response to light (Fig. S5).

To investigate if also plastid gene expression is affected in the *bzip* triple mutant, we analyzed the expression of six chloroplast encoded genes which are transcribed by PEP. These genes encode for proteins associated with the photosynthetic electron transport chain including PSII (*psbD*), cytochrome b6f complex (*petB*), PSI (*psaA*), ATP synthase (*atpA*), NADH dehydrogenase (*ndhF*) and we also included the large subunit of Rubisco (*rbcL*). Following exposure to 24 h of light, all these genes were significantly downregulated in the *bzip* triple mutant compared to WT (Fig. 2e). Taken together, our analyses of gene expression suggest that the bZIP16, bZIP68 and GBF1 proteins are involved in the regulation of photosynthesis-related genes in response to light and the misregulation of these genes in the *bzip* triple mutant could subsequently cause the delayed de-etiolation phenotype.

The bZIP proteins mediate blue light signaling possibly through interaction with cryptochrome.

CRY1 and 2 regulates the expression of up to 20% of the nuclear genes in response to blue light (Ma et al., 2001) and several studies have proposed that CRYs may affect gene expression by binding to DNA, direct interaction with DNA binding factors or indirectly by affecting other proteins regulating the activity of transcriptional regulators (Pedmale et al., 2016; Ma et al., 2016; Wang et al., 2018; Griffin et al., 2020). To further assess the function of bZIP16, bZIP68 and GBF1 in response to light, we analyzed the expression of *LHCBI.1* following exposure to 20 $\mu\text{mol/m/s}$ blue or red light for 12 and 24 h. The expression of *LHCBI.1* was strongly induced following 12 h in both blue and red-light conditions similar to that in white light (Fig. 3a; S6a). However, while the expression of *LHCBI.1* was significantly down regulated in the *bzip* triple mutant under blue light, there was no difference compared to wild type under red light condition (Fig. 3a; S6a). This suggests that the bZIP proteins mediate blue light response to control the expression of *LHCBI.1*, while under red light conditions other components are responsible for the *LHCBI.1* expression. Thus, we analyzed *SIG1* and *SIG5* expression following 20 $\mu\text{mol/m/s}$ blue light exposure for 12 and 24 h. Under white light, both *SIG1* and *SIG5* expression was down regulated

in the *bzip* triple mutant (Fig. 2d), but under blue light, only *SIG5* expression was down regulated and not *SIG1* (Fig. 3b; S6b). This suggests that under the 20 $\mu\text{mol/m/s}$ blue light condition, *SIG1* is not regulated by bZIP16, bZIP68 and GBF1 in contrast to *SIG5*. The explanation for this difference could lie in the fact that the induction of *SIG1* and *SIG5* in blue light is not regulated in the same manner. At fluences greater than 10 $\mu\text{mol/m/s}$ blue light, a *SIG5*-specific second phase induction has been described that does not occur for *SIG1* expression (Onda et al., 2008). Thus, the bZIPs regulate *SIG1* expression under the white light condition used in this study, but under 20 $\mu\text{mol/m/s}$ blue light condition other components regulate *SIG1* expression. As observed in white light, there was no significant difference between wild type and *bzip* triple mutant in the expression profiles of *SIG2*, 3, 4 and 6 in response to blue light (Fig. S6c–f).

The potential function of bZIP16, bZIP68 and GBF1 in mediating blue light signals suggests that there is an interaction with the cryptochrome photoreceptor pathways. To explore this further we retrieved available RNA-sequencing data in which CRY1 and CRY2 regulated genes were identified (He et al., 2015). This dataset of 3436 CRY-regulated genes was compared to the total identified 6996 target genes from bZIP16 and bZIP68 DAP-sequencing analyses combined. We found that almost one third of the CRY-regulated genes (1030 genes) are also targets of bZIP16 and/or bZIP68 (Fig. 3c, Table S3). GO term enrichment analysis was performed using these 1030 overlapping genes to identify terms with significant enrichment (FDR<0.05). While for the biological process, the top terms included different categories such as responses to abiotic stimuli, photosynthesis, light stimulus, stress, and hormone (Fig. S7a), the cellular component terms clearly demonstrate that the common genes between CRYs and these bZIPs are targeted to the chloroplast (Fig. 3c, Table S3).

While the cryptochromes evidently have overlapping functions, CRY1 primarily mediates blue light regulation of de-etiolation and CRY2 the photoperiodic control of flowering (Ahmad & Cashmore, 1993; Guo et al., 1998). In addition, while CRY2 undergoes ubiquitination and is degraded immediately by the 26S proteasome system under blue light conditions, CRY1 get degraded only in response to strong blue light (Batschauer, 2022). Thus, CRY1 is the potential photoreceptor that could be involved in the regulation of the bZIP transcription activity in response to light and we tested if CRY1 interacts with the bZIP proteins. We co-infiltrated Flag-CRY1 with either bZIP16-Myc, bZIP68-Myc or GBF1-Myc in *Nicotiana benthamiana* leaves and analyzed for co-immunoprecipitation (Co-IP). The IP was performed using Myc-tagged magnetic beads and the immunoblot analysis showed that the bZIP16-Myc, bZIP68-Myc and GBF1-Myc proteins physically interact with Flag-CRY1 (Fig. 3d), however, bZIP16/bZIP68/GBF1-Myc alone did not co-purify during the pulldown. We also used a second method, a split LUC assay to confirm the interaction between CRY1 and bZIP16. The split LUC assay is specific for a direct interaction between the two proteins (Supplementary Figure S7b). Protoplasts were transfected with constructs for CRY1n, CRY1c, bZIP16n and bZIP16c in all different combinations. Following the transfection, the protoplasts were exposed to 16 h blue light and LUC activity was detected. Significant LUC activity was detected for the positive controls, CRY1c-CRY1n and bZIP16c-bZIP16n which was expected as both bZIP16 and CRY1 form dimers. LUC activity was also detected for the combination bZIP16c-CRY1n whereas no LUC activity

was detected for the combinations bZIP16n-CRY1n. Taken together, interaction between CRY1-bZIP was detected with two different approaches and using two different systems, tobacco and Arabidopsis, indicating that the bZIP proteins may be directly regulated by CRY1. We further explored if the interaction between bZIPs and CRY1 was stimulated by BL. *Nicotiana benthamiana* leaves were infiltrated with constructs for CRY1n, CRY1c, bZIP16n and bZIP16c. We also included a negative control as CDK8c was co-infiltrated with CRY1n or bZIP16n. The leaves were kept in the dark following the transfection for 5 hours and then shifted to BL for 10 minutes. As a positive control the leaves were kept in light following the transfection (Supplementary Figure S7c). Expression of the different LUC-fusion proteins was confirmed with Western blot (Supplementary Figure S7d). No interaction could be detected between CDK8 and bZIP16 or CRY1 (Fig. 3e, S7c). Although an interaction was observed in the dark, the interaction between bZIP16 and CRY1 was significantly stimulated by BL exposure (Fig. 3e) whereas the dimerization of bZIP16 and CRY1 was not BL stimulated under these conditions (Fig. 3e) (Yu et al., 2010). A significant BL stimulation of the CRY1 bZIP interaction was observed in two independent experiments.

A genetic interaction was also observed between CRYs and the bZIPs as the *cry1cry2* double mutation is epistatic to the *cry1cry2bzip16bzip68gbf1* (*crybzip*) quintuple mutant regarding *LHCBI.1* expression in response to blue light (Fig. 4a). We also performed an analysis of cotyledon opening using the *bzip* triple, *cry1cry2* double and *cry1cry2bzip16bzip68gbf1* (*crybzip*) quintuple mutants. The seedlings were scanned in the dark and following exposure to light for a time series up to 24 h and analyzed for the cotyledon opening. Cotyledon opening was delayed in the *bzip* triple mutant, but the effect was significantly stronger in the *cry1cry2* double mutant (Fig. 4b). Similar to the expression of *LHCBI.1*, *cry1cry2* double mutation was epistatic to the *cry1cry2bzip16bzip68gbf1* (*crybzip*) quintuple mutant for cotyledon opening (Fig. 4b). Taken together, the genetic data further supports that the bZIPs and CRY1/2 function in the same pathway.

Activity of bZIP16 is mediated via Cys330.

The binding specificity of bZIP proteins to DNA has been shown to be a result of both variations of the *cis*-element and its flanking nucleotides, and variability of the binding region of the protein (Llorca et al., 2014). Certainly, many of the bZIPs recognize the same DNA sequences and have redundant functions, however, extensive regulation of the bZIP proteins themselves give rise to specific functions and responses to specific signals. The regulation of bZIP proteins includes for instance transcriptional/translational control, dimerization properties and post-translational control. To further understand how the bZIP16, bZIP68 and GBF1 proteins themselves are regulated during the de-etiolation process, we analyzed the expression of the bZIP genes in response to light. Following 12 and 24 h of exposure to light there was no significant change in expression of the *bZIP16*, *bZIP68* and *GBF1* genes, indicating that these transcription factors most likely are regulated on posttranslational level (Fig. S8a).

It has previously been reported that the DNA-binding activity of bZIP16, bZIP68, and GBF1 is regulated by redox changes (Shaikhali et al., 2012). These bZIP proteins contain two cysteine residues each in their protein sequence, and one of these residues is conserved

within the bZIP domain (Supplementary Figure S9) (Shaikhali et al., 2012). For bZIP16, the cysteine residues are located in position 330 (C1) and 358 (C2) (Fig. 5a). The formation or breakage of disulfide bonds between cysteine residues in proteins is a key modification for responses to redox changes and for modifying protein activity (Amoutzias et al., 2006; Marchal et al., 2014). It was demonstrated that the conserved cysteine residue (bZIP16 C330, bZIP68 C320 and GBF1 C247) is responsible for intermolecular disulfide bridges between bZIP monomers. In a theoretical model, bZIP16 Cys330 was positioned at the domain between the leucine zipper and the basic DNA-binding region, just outside the DNA contact sites (Shaikhali et al., 2012). In the reduced form, the disulfide bridge is disrupted which forms an open conformation of the bZIP zipper that allows DNA binding, while when the disulfide bond is formed under oxidized conditions the zipper is not flexible enough to allow DNA binding (Fig. 5a).

To investigate if the bZIP cysteine residues are involved in the regulation of gene expression during de-etiolation, we overexpressed the bZIP16 WT protein and mutated versions of the bZIP16 cysteines to leucine (bZIP16 C330L and bZIP16 C358L) in the *bzip* triple mutant background (Fig. S8b). Etiolated seedlings of these overexpressing lines were scanned in dark and following exposure to light during 12 h and analyzed for the cotyledon opening. The result demonstrates that the cotyledon opening was significantly delayed in the *bZIP16 C330L* overexpressing line compared to *bZIP16 WT* at 3, 6, 9 and even 12 h of light exposure (Fig. 5b). The *bZIP16 C358L* overexpressing line followed a similar development as the *bZIP16 WT* seedlings and showed a significantly enhanced cotyledon opening following 9 and 12 h of light exposure (Fig. 5b). We also analyzed the expression of the *LHCB1.1* and *LHCB2.4* genes in the *bZIP16 WT*, *C330L* and *C358L* lines and both of these genes are strongly down regulated in the *bZIP16 C330L* line following 12 h of light exposure compared to the *bZIP16 WT* and *C358L* lines (Fig. 5c, d). While there was no effect of the bZIP16 C358L mutation compared to WT regarding *LHCB* expression. These results show that the overexpression of bZIP16 C330L, which cannot form the disulfide bond and thereby promotes DNA binding, causes delayed de-etiolation and down regulated *LHCB* expression, suggesting that bZIP16 acts as a repressor during the de-etiolation process. While the *bzip* single mutants did not display any visible phenotype during de-etiolation (Fig. S2b), *LHCB2.4* expression in the *bzip16* single mutant was significantly higher compared to WT (Fig. S10b) supporting a role for bZIP16 as a repressor. We also investigated the *bzip68gbf1* double mutant and whether the exclusion of these two potential activators is enough to cause an effect on *LHCB* expression during de-etiolation. Expression of *LHCB1.1* and *LHCB2.4* in the *bzip68gbf1* mutant was not different from WT, indicating that the exclusion of these two bZIPs is not enough to cause the phenotype observed in the *bzip* triple mutant (Fig. S10a, b). In addition, either the *bzip16* or the *bzip68gbf1* seedlings displayed any visible phenotype compared to WT (Fig. S10c). These results suggest that a complex interplay between the three bZIPs controls gene expression during photomorphogenesis.

Discussion

Light is indispensable for plants and promotes the onset of photomorphogenic growth in seedlings. The initial light exposure induces major redox changes within the plant cell, and

the balance between utilization of light energy and protection against oxidative damage is crucial. Here we investigated the activity of three bZIP proteins during dark to light transition and show that they play an important function in the delicate regulation of photosynthesis-related nuclear genes during the early light hours. The activity of bZIP16 is dependent on a cysteine residue which is conserved among bZIP16, bZIP68 and GBF1, indicating a redox-mediated regulation of these bZIP proteins that is critical to the de-etiolation process.

bZIP16, bZIP68, and GBF1 are known to preferentially bind to the G-box *cis*-element which has been identified in promoters of genes that are both induced and repressed in response to light, suggesting interactions with transcription factors acting both as activators and repressors (Kleine et al., 2007). Transcriptome analysis has showed that bZIP16 primarily functions as a transcriptional repressor in dark (Hsieh et al., 2012). GBF1 has been described as both a positive and negative regulator in photomorphogenic growth and gene expression. For instance, GBF1 has been shown to be required for proper activation of *LHCB* expression but acts as a negative regulator of *RBCS* expression (Mallappa et al., 2006). bZIP68 was reported to suppress expression of stress tolerance genes and promote expression of growth-related genes (Li et al., 2019). In a previous study the *bzip68* and *gbf1* mutants, and a bZIP16 overexpressing line all showed down regulated *LHCB* expression in 5-day-old seedlings grown continuous white light (Shaikhali et al., 2012), suggesting that bZIP16 functions as a repressor while bZIP68 and GBF1 are activators of *LHCB*. A repressing function of bZIP16 is in concert with the result that the overexpression of *bZIP16 C330L*, which is the active DNA binding form, causes repressed *LHCB* expression during de-etiolation (Fig. 5c, d). In the *bzip* triple mutant, we observed down regulated *LHCB* expression compared to WT (Fig. 2b, c). Reduced expression was also observed for the *SIG1* and *SIG5* genes (Fig. 2d, Fig. S4a, e). This suggests that while bZIP16 functions as a repressor of *PhANG* expression during de-etiolation, bZIP68/GBF1 act as activators. However, the generated *bzip68gbf1* double mutant demonstrates that the exclusion of these two bZIPs is not enough to cause the delayed de-etiolation phenotype, and in the *bzip16* mutant only *LHCB2.4* expression was affected (Fig. S10). This demonstrates that these three bZIP proteins depend upon each other and act together during de-etiolation to regulate the expression of nuclear genes.

Another level of complexity when it comes to the bZIP transcription factors is their ability to form heterodimers. The formation of both homo- and heterodimers has been shown for instance within the G-group (Shen et al., 2008; Shaikhali et al., 2012) and the H-group of bZIP transcription factors (Holm et al., 2002). Also, interactions between members of different groups have been shown for instance for the A-group bZIP G-box Binding Factor 4 (GBF4) and members of the G-group (Menkens & Cashmore, 1994). The H-group members HY5 and HYH can interact with GBF1, and the interactions between GBF1, HY5 and HYH play a role during light-regulated gene expression and photomorphogenesis (Singh et al., 2012; Ram et al., 2014). Each of these proteins can form homodimers which bind to the G-box *cis*-element. However, the formation of heterodimers between GBF1 and HY5 increases their binding affinity to DNA, while the GBF1-HYH heterodimer is unable to bind to the G-box. There is also a possibility for interaction between bZIP16/bZIP68 and HY5 and there is a significant overlap between bZIP16/bZIP68 and HY5 target genes

(Supplemental table S4). Thus, heterodimerization of bZIP16, bZIP68 and GBF1 with each other or additional bZIP proteins could be a potential mechanism *in vivo* to generate positive and negative regulators, which in turn may play opposite roles for light-regulated gene expression and seedling development. Despite the relatively strong initial phenotype in the *bzip* triple mutant following a dark-to-light shift, the seedlings eventually manage to recover and induce photomorphogenic growth as indicated by the phenotype after 96 h in light (Fig. 1a–c). This indicates that the exclusion of all three bZIP proteins in the triple mutant would free up the G-box binding sites and allow other G-box binding factors to eventually bind and induce the required gene expression. Thus, later during the de-etiolation process other transcription factors appear to play the primary role as the phenotype of the *bzip* triple mutant is basically undistinguishable from wild type following 96 hours of light exposure.

It was previously demonstrated that bZIP16, bZIP68 and GBF1 are redox regulated by the formation of disulfide bonds between a conserved cysteine residue (Shaikhali et al., 2012). A sequence comparison among all plant bZIP proteins revealed that the cysteine residue at this specific location is present only in the G-group members bZIP16, bZIP68 and GBF1 (Shaikhali et al., 2012), and is not conserved among the two G-group members GBF2 and GBF3. A sequence comparison among all Arabidopsis bZIP proteins revealed that this specific cysteine is also present in bZIP62 (Fig. S9a). bZIP62 is not grouped together with any of the other bZIP proteins as proposed in Jakoby et al. (2002), but a phylogenetic analysis demonstrated that the closest homologues are the G-group proteins (Fig. S9b). The activity of bZIP16 during de-etiolation is dependent on the conserved Cys330 residue as shown by the bZIP16 mutated lines (Figure 5). This Cys330 residue has been linked to redox regulation of the DNA binding (Shaikhali et al., 2012) as mutant variants of bZIP16 with the inability to form disulfide bonds significantly increased DNA binding activity (Shaikhali et al., 2012). The demonstrated interaction between CRY1 and bZIP16, bZIP68 and GBF1 allows us to postulate that the electrons most likely come from CRY1. Such a light triggered mechanism of redox regulation of the bZIP16, bZIP68 and GBF1 proteins could be the prerequisite to their important role during early light signaling. During dark-to-light transition, seedlings face changes in redox status that potentially affect redox regulated proteins. The function of bZIP16 in the regulation of cotyledon opening and *LHCB* expression was shown to be dependent on the conserved cysteine residue (Fig. 5a–d). The activity of both repressors and activators is a prerequisite to balance and coordinate gene expression between the nucleus and plastids, for instance not to produce an excess of light harvesting proteins before the complete electron transfer chain is established. Possibly, bZIP68/GBF1 compete out bZIP16 to induce the initial expression of *PhANGs*, or a delicate interplay between these three bZIPs promotes just the right amount of gene expression to avoid photooxidative damage during the first light hours.

The *bzip* triple mutant show strongly attenuated expression of the plastid encoded genes associated with photosynthesis (Fig. 2e). The downregulation observed for *SIG1* and *SIG5* may not be the sole cause of this, and it is more likely a combined effect of the down regulation of other nuclear genes involved in photomorphogenesis (Fig. 2b, c; Fig. S5), less accumulation of chlorophyll (Fig. 1c), and delayed chloroplast development (Fig. 1d–g). A recently performed bioinformatical study has analyzed the influence of photoreceptors in the control of nuclear genes with a function in the chloroplast. This study

emphasizes a genome-wide role of cryptochromes and phytochromes in the modulation of the chloroplast, including genes both in the nuclear and plastid, whose products act for the onset of photosynthesis, plastid development and for the production of plastid essential metabolites (Griffin et al., 2020). The bZIP16 and bZIP68 target genes overlap with one third of genes regulated by cryptochromes, and the bZIPs regulate gene expression in a blue light-dependent manner (Fig. 3). This indicates that the bZIPs function in cryptochrome-mediated signal transduction. The mechanisms of CRY signaling in plants primarily involves protein-protein interactions. Photoactivation of inactive CRY monomers leads to conformational change and homooligomerization which allows interaction with downstream proteins (Wang & Lin, 2020). Some of the known CRY interactors are the COP1/SPA complex, phytochrome-interacting factors (PIFs) and cryptochrome-interacting basic-helix-loop-helix (CIB) transcription factors, but most proteins present in the CRY complexes are believed to be unknown to date (Wang & Lin, 2020).

The demonstrated BL stimulated interaction between CRY1 and bZIPs provides a possible answer to how these bZIP proteins can be regulated in response to light signals (Fig. 3e). Flavin adenine dinucleotide (FAD) is the chromophore cofactor that is responsible for cryptochrome photosensing. Absorption of a photon of light energy leads to the formation of the light activated radical or reduced flavin ($FAD^{\bullet}/FADH^{-}$), which is subsequently reoxidized back to the resting state (Muller & Ahmad, 2011). It has been further shown that the reoxidation of reduced FAD occurs via cleavage of molecular oxygen (O_2) and results in the formation of reactive oxygen species (ROS) including hydrogen peroxide (H_2O_2) and superoxide ($O_2^{\bullet-}$) (Consentino et al., 2015). At this point we do not know how CRY1 might affect the activity of bZIP16 in response to light, but the redox changes sensed and mediated by FAD could possibly also affect CRY interactors. Initially CRY1 might reduce and activate the bZIPs, while in extended blue light, ROS is formed and the bZIPs could be oxidized and inactivated which could explain the discrete temporal role of the bZIPs during the early light response. However, exploring this further is an exciting scope for future investigations using various transactivation assays where the specific conditions can be controlled.

Supplementary Material

Refer to Web version on PubMed Central for supplementary material.

Acknowledgements:

This work was supported by grants from the Swedish research foundation, VR (Å.S.), National Institutes of Health (NIH) grant R35GM125003 (U.V.P.).

Data availability.

All data supporting the findings of this work are available within the paper and supplemental information.

References

- Ahmad M, Cashmore AR. 1993. Hy4 Gene of *a-Thaliana* Encodes a Protein with Characteristics of a Blue-Light Photoreceptor. *Nature* 366(6451): 162–166. [PubMed: 8232555]
- Allen JF, de Paula WBM, Puthiyaveetil S, Nield J. 2011. A structural phylogenetic map for chloroplast photosynthesis. *Trends in Plant Science* 16(12): 645–655. [PubMed: 22093371]
- Amoutzias GD, Bornberg-Bauer E, Oliver SG, Robertson DL. 2006. Reduction/oxidation-phosphorylation control of DNA binding in the bZIP dimerization network. *BMC Genomics* 7: 107. [PubMed: 16674813]
- Bartlett A, O'Malley RC, Huang SSC, Galli M, Nery JR, Gallavotti A, Ecker JR. 2017. Mapping genome-wide transcription-factor binding sites using DAP-seq. *Nature Protocols* 12(8): 1659–1672. [PubMed: 28726847]
- Batschauer A. 2022. New insights into the regulation of *Arabidopsis* cryptochrome 1. *New Phytologist* 234(4): 1347–1362. [PubMed: 34449898]
- Chen H, Zou Y, Shang Y, Lin H, Wang Y, Cai R, Tang X, Zhou JM. 2008. Firefly Luciferase Complementation Imaging Assay for Protein-Protein Interactions in Plants. *Plant Physiology*, 146(2): 323–324.
- Chen M, Chory J, Fankhauser C. 2004. Light signal transduction in higher plants. *Annual Review of Genetics* 38: 87–117.
- Chi W, He BY, Mao J, Jiang JJ, Zhang LX. 2015. Plastid sigma factors: Their individual functions and regulation in transcription. *Biochimica Et Biophysica Acta-Bioenergetics* 1847(9): 770–778.
- Clough SJ, Bent AF. 1998. Floral dip: a simplified method for *Agrobacterium*-mediated transformation of *Arabidopsis thaliana*. *Plant Journal* 16(6): 735–743.
- Consentino L, Lambert S, Martino C, Jourdan N, Bouchet PE, Witczak J, Castello P, El-Esawi M, Corbineau F, d'Harlingue A, et al. 2015. Blue-light dependent reactive oxygen species formation by *Arabidopsis* cryptochrome may define a novel evolutionarily conserved signaling mechanism. *New Phytologist* 206(4): 1450–1462. [PubMed: 25728686]
- Dubreuil C, Jin X, Barajas-Lopez JD, Hewitt TC, Tanz SK, Dobrenel T, Schroder WP, Hanson J, Pesquet E, Gronlund A, et al. 2018. Establishment of Photosynthesis through Chloroplast Development Is Controlled by Two Distinct Regulatory Phases. *Plant Physiology* 176(2): 1199–1214. [PubMed: 28626007]
- Galvao VC, Fankhauser C. 2015. Sensing the light environment in plants: photoreceptors and early signaling steps. *Current Opinion in Neurobiology* 34: 46–53. [PubMed: 25638281]
- Giri MK, Singh N, Banday ZZ, Singh V, Ram H, Singh D, Chattopadhyay S, Nandi AK. 2017. GBF1 differentially regulates CAT2 and PAD4 transcription to promote pathogen defense in *Arabidopsis thaliana*. *Plant Journal* 91(5): 802–815.
- Griffin JHC, Prado K, Sutton P, Toledo-Ortiz G. 2020. Coordinating light responses between the nucleus and the chloroplast, a role for plant cryptochromes and phytochromes. *Physiologia Plantarum* 169(4): 515–528. [PubMed: 32519399]
- Guo H, Yang H, Mockler TC, Lin C. 1998. Regulation of flowering time by *Arabidopsis* photoreceptors. *Science* 279(5355): 1360–1363. [PubMed: 9478898]
- Hanaoka M, Kanamaru K, Takahashi H, Tanaka K. 2003. Molecular genetic analysis of chloroplast gene promoters dependent on SIG2, a nucleus-encoded sigma factor for the plastid-encoded RNA polymerase, in *Arabidopsis thaliana*. *Nucleic Acids Research* 31(24): 7090–7098. [PubMed: 14654684]
- He SB, Wang WX, Zhang JY, Xu F, Lian HL, Li L, Yang HQ. 2015. The CNT1 Domain of *Arabidopsis* CRY1 Alone Is Sufficient to Mediate Blue Light Inhibition of Hypocotyl Elongation. *Molecular Plant* 8(5): 822–825. [PubMed: 25721730]
- Hedtke B, Borner T, Weihe A. 1997. Mitochondrial and chloroplast phage-type RNA polymerases in *Arabidopsis*. *Science* 277(5327): 809–811. [PubMed: 9242608]
- Holm M, Ma LG, Qu LJ, Deng XW. 2002. Two interacting bZIP proteins are direct targets of COP1-mediated control of light-dependent gene expression in *Arabidopsis*. *Genes & Development* 16(10): 1247–1259. [PubMed: 12023303]

- Hsieh WP, Hsieh HL, Wu SH. 2012. Arabidopsis bZIP16 Transcription Factor Integrates Light and Hormone Signaling Pathways to Regulate Early Seedling Development. *Plant Cell* 24(10): 3997–4011. [PubMed: 23104829]
- Hu J, Bogorad L. 1990. Maize Chloroplast Rna-Polymerase - the 180-Kilodalton, 120-Kilodalton, and 38-Kilodalton Polypeptides Are Encoded in Chloroplast Genes. *Proceedings of the National Academy of Sciences of the United States of America* 87(4): 1531–1535. [PubMed: 2304916]
- Hur YS, Kim J, Kim S, Son O, Kim WY, Kim GT, Ohme-Takagi M, Cheon CI. 2019. Identification of TCP13 as an Upstream Regulator of ATHB12 during Leaf Development. *Genes (Basel)* 10 (9): 644. [PubMed: 31455029]
- Jakoby M, Weisshaar B, Droge-Laser W, Vicente-Carbajosa J, Tiedemann J, Kroj T, Parcy F, b ZIPRG. 2002. bZIP transcription factors in Arabidopsis. *Trends in Plant Science* 7(3): 106–111. [PubMed: 11906833]
- Jarvis P, Lopez-Juez E. 2013. Biogenesis and homeostasis of chloroplasts and other plastids. *Nature Reviews Molecular Cell Biology* 14(12): 787–802. [PubMed: 24263360]
- Kleine T, Kindgren P, Benedict C, Hendrickson L, Strand A. 2007. Genome-wide gene expression analysis reveals a critical role for CRYPTOCHROME1 in the response of Arabidopsis to high irradiance. *Plant Physiology* 144(3): 1391–1406. [PubMed: 17478635]
- Lee J, He K, Stolc V, Lee H, Figueroa P, Gao Y, Tongprasit W, Zhao H, Lee I, Deng XW. 2007. Analysis of transcription factor HY5 genomic binding sites revealed its hierarchical role in light regulation of development. *Plant Cell* 19(3): 731–749. [PubMed: 17337630]
- Li Y, Liu W, Zhong H, Zhang HL, Xia Y. 2019. Redox-sensitive bZIP68 plays a role in balancing stress tolerance with growth in Arabidopsis. *Plant Journal* 100(4): 768–783.
- Llorca CM, Potschin M, Zentgraf U. 2014. bZIPs and WRKYs: two large transcription factor families executing two different functional strategies. *Frontiers in Plant Science* 5: 169. [PubMed: 24817872]
- Luo XM, Lin WH, Zhu S, Zhu JY, Sun Y, Fan XY, Cheng M, Hao Y, Oh E, Tian M, Liu L, Zhang M, Xie Q, Chong K, Wang ZY. 2010. Integration of Light- and Brassinosteroid-Signaling Pathways by a GATA Transcription Factor in Arabidopsis. *Developmental Cell* 19(6): 872–883. [PubMed: 21145502]
- Ma D, Li X, Guo Y, Chu J, Fang S, Yan C, Noel JP, Liu H. 2016. Cryptochrome 1 interacts with PIF4 to regulate high temperature-mediated hypocotyl elongation in response to blue light. *Proc. Natl. Acad. Sci. USA* 113:224–229. [PubMed: 26699514]
- Ma LG, Li JM, Qu LJ, Hager J, Chen ZL, Zhao HY, Deng XW. 2001. Light control of Arabidopsis development entails coordinated regulation of genome expression and cellular pathways. *Plant Cell* 13(12): 2589–2607. [PubMed: 11752374]
- Mallappa C, Singh A, Ram H, Chattopadhyay S. 2008. GBF1, a transcription factor of blue light signaling in Arabidopsis, is degraded in the dark by a proteasome-mediated pathway independent of COP1 and SPA1. *Journal of Biological Chemistry* 283(51): 35772–35782. [PubMed: 18930926]
- Mallappa C, Yadav V, Negi P, Chattopadhyay S. 2006. A basic leucine zipper transcription factor, G-box-binding factor 1, regulates blue light-mediated photomorphogenic growth in Arabidopsis. *Journal of Biological Chemistry* 281(31): 22190–22199. [PubMed: 16638747]
- Marchal C, Delorme-Hinoux V, Bariat L, Siala W, Belin C, Saez-Vasquez J, Riondet C, Reichheld JP. 2014. NTR/NRX define a new thioredoxin system in the nucleus of Arabidopsis thaliana cells. *Mol Plant* 7(1): 30–44. [PubMed: 24253198]
- Maurya JP, Sethi V, Gangappa SN, Gupta N, Chattopadhyay S. 2015. Interaction of MYC2 and GBF1 results in functional antagonism in blue light-mediated Arabidopsis seedling development. *Plant Journal* 83(3): 439–450.
- Menkens AE, Cashmore AR. 1994. Isolation and characterization of a fourth Arabidopsis thaliana G-box-binding factor, which has similarities to Fos oncoprotein. *Proc Natl Acad Sci U S A* 91(7): 2522–2526. [PubMed: 8146148]
- Muller P, Ahmad M. 2011. Light-activated cryptochrome reacts with molecular oxygen to form a flavin-superoxide radical pair consistent with magnetoreception. *Journal of Biological Chemistry* 286(24): 21033–21040. [PubMed: 21467031]

- O'Malley RC, Huang SSC, Song L, Lewsey MG, Bartlett A, Nery JR, Galli M, Gallavotti A, Ecker JR. 2016. Cistrome and Epicistrome Features Shape the Regulatory DNA Landscape (vol 165, pg 1280, 2016). *Cell* 166(6): 1598–1598. [PubMed: 27610578]
- Onda Y, Yagi Y, Saito Y, Takenaka N, Toyoshima Y. 2008. Light induction of Arabidopsis SIG1 and SIG5 transcripts in mature leaves: differential roles of cryptochrome 1 and cryptochrome 2 and dual function of SIG5 in the recognition of plastid promoters. *Plant Journal* 55(6): 968–978.
- Pedmale UV, Huang SSC, Zander M, Cole BJ, Hetzel J, Ljung K, Reis PAB, Sridevi P, Nito K, Nery JR, et al. 2016. Cryptochromes Interact Directly with PIFs to Control Plant Growth in Limiting Blue Light. *Cell* 164(1–2): 233–245. [PubMed: 26724867]
- Pfaffl MW. 2001. A new mathematical model for relative quantification in real-time RT-PCR. *Nucleic Acids Research* 29(9).
- Pogson BJ, Albrecht V. 2011. Genetic Dissection of Chloroplast Biogenesis and Development: An Overview. *Plant Physiology* 155(4): 1545–1551. [PubMed: 21330494]
- Porra RJ, Thompson WA, Kriedemann PE. 1989. Determination of Accurate Extinction Coefficients and Simultaneous-Equations for Assaying Chlorophyll-a and Chlorophyll-B Extracted with 4 Different Solvents - Verification of the Concentration of Chlorophyll Standards by Atomic-Absorption Spectroscopy. *Biochimica Et Biophysica Acta* 975(3): 384–394.
- Ram H, Priya P, Jain M, Chattopadhyay S. 2014. Genome-wide DNA binding of GBF1 is modulated by its heterodimerizing protein partners, HY5 and HYH. *Mol Plant* 7(2): 448–451. [PubMed: 24157608]
- Ramakers C, Ruijter JM, Deprez RHL, Moorman AFM. 2003. Assumption-free analysis of quantitative real-time polymerase chain reaction (PCR) data. *Neuroscience Letters* 339(1): 62–66. [PubMed: 12618301]
- Romand S, Abdelkefi H, Lecampion C, Belaroussi M, Dussenne M, Ksas B, Citerne S, Caius J, D'Alessandro S, Fakhfakh H, Caffarri S, Havaux M, Field B. 2022. A guanosine tetraphosphate (ppGpp) mediated brake on photosynthesis is required for acclimation to nitrogen limitation in Arabidopsis. *eLife* 11: e75041. [PubMed: 35156611]
- Schindelin J, Arganda-Carreras I, Frise E, Kaynig V, Longair M, Pietzsch T, Preibisch S, Rueden C, Saalfeld S, Schmid B, et al. 2012. Fiji: an open-source platform for biological-image analysis. *Nature Methods* 9(7): 676–682. [PubMed: 22743772]
- Schindler U, Terzaghi W, Beckmann H, Kadesch T, Cashmore AR. 1992. DNA binding site preferences and transcriptional activation properties of the Arabidopsis transcription factor GBF1. *Embo Journal* 11(4): 1275–1289. [PubMed: 1563344]
- Shaikhali J, Noren L, de Dios Barajas-Lopez J, Srivastava V, Konig J, Sauer UH, Wingsle G, Dietz KJ, Strand A. 2012. Redox-mediated mechanisms regulate DNA binding activity of the G-group of basic region leucine zipper (bZIP) transcription factors in Arabidopsis. *Journal of Biological Chemistry* 287(33): 27510–27525. [PubMed: 22718771]
- Shen H, Cao K, Wang X. 2008. AtbZIP16 and AtbZIP68, two new members of GBFs, can interact with other G group bZIPs in Arabidopsis thaliana. *BMB Rep* 41(2): 132–138. [PubMed: 18315949]
- Siberil Y, Doireau P, Gantet P. 2001. Plant bZIP G-box binding factors. Modular structure and activation mechanisms. *Eur J Biochem* 268(22): 5655–5666. [PubMed: 11722549]
- Singh A, Ram H, Abbas N, Chattopadhyay S. 2012. Molecular interactions of GBF1 with HY5 and HYH proteins during light-mediated seedling development in Arabidopsis thaliana. *Journal of Biological Chemistry* 287(31): 25995–26009. [PubMed: 22692212]
- Smykowski A, Fischer SM, Zentgraf U. 2015. Phosphorylation Affects DNA-Binding of the Senescence-Regulating bZIP Transcription Factor GBF1. *Plants (Basel)* 4(3): 691–709. [PubMed: 27135347]
- Wang Q, Lin C. 2020. Mechanisms of Cryptochrome-Mediated Photoresponses in Plants. *Annual Review of Plant Biology* 71: 103–129.
- Wang Q, Sullivan RW, Kight A, Henry RL, Huang J, Jones AM, Korth KL. 2004. Deletion of the Chloroplast-Localized Thylakoid Formation1 Gene Product in Arabidopsis Leads to Deficient Thylakoid Formation and Variegated Leaves. *Plant Physiol* 136 (3): 3594–3604. [PubMed: 15516501]

- Wang W, Lu X, Li L, Lian H, Mao Z, Xu P, Guo T, Xu F, Du S, Cao X, Wang S, Shen H, Yang HQ. 2018. Photoexcited CRYPTOCHROME1 interacts with dephosphorylated BES1 to regulate brassinosteroid signaling and photomorphogenesis in Arabidopsis. *Plant Cell* 30: 1989–2005. [PubMed: 30131420]
- Yoo SD, Cho YH, Sheen J. 2007. Arabidopsis mesophyll protoplasts: A versatile cell system for transient gene expression analysis. *Nature Protocols*, 2(7): Article 7.
- Yu G, Xian L, Xue H, Yu W, Rufian JS, Sang Y, Morcillo RJL, Wang Y, Macho AP. 2020. A bacterial effector protein prevents MAPK-mediated phosphorylation of SGT1 to suppress plant immunity. *PLoS Pathogens*, 16(9): e1008933. [PubMed: 32976518]
- Yu X, Liu H, Klejnot J, Lin C. 2010. The Cryptochrome Blue Light Receptors. *Arabidopsis Book*, 8:e0135. [PubMed: 21841916]

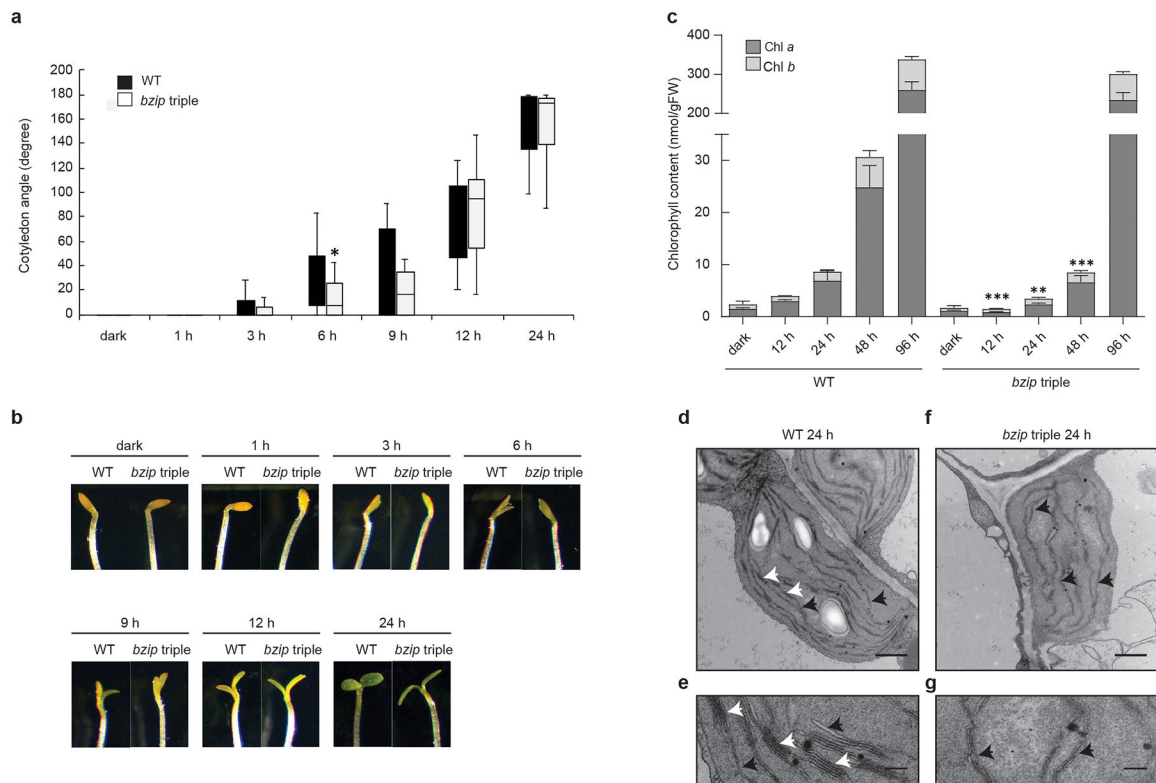


Figure 1. De-etiolation is delayed in the *bzip* triple mutant.

Etiolated seedlings of Arabidopsis WT and *bzip* triple mutant were exposed to white light and (a) scanned to measure the cotyledon opening. Each data point represents the mean (\pm SD) of at least 25 seedlings. The *bzip* triple mutant was significantly different from WT at 6 h of light exposure as demonstrated by Student *t*-test: * $p < 0.05$. (b) Representative seedlings were photographed for each genotype and time point to demonstrate the observed phenotype during the cotyledon opening experiment. (c) Seedlings were sampled and analyzed for chlorophyll a and b content. Each data point represents the mean (\pm SD) of at least 4 biological replicates. (d-g) Representative transmission electron microscopy (TEM) images of chloroplasts of WT and *bzip* triple seedlings following 24 h of light exposure. (d and f) Images of the chloroplasts showing the thylakoid arrangement (scale bar = 1 μ m). (e and g) Higher magnification showing the grana stacking arrangement (scale bar = 200 nm). Black arrowheads point at internal thylakoid membranes and white arrowheads point at grana stacks.

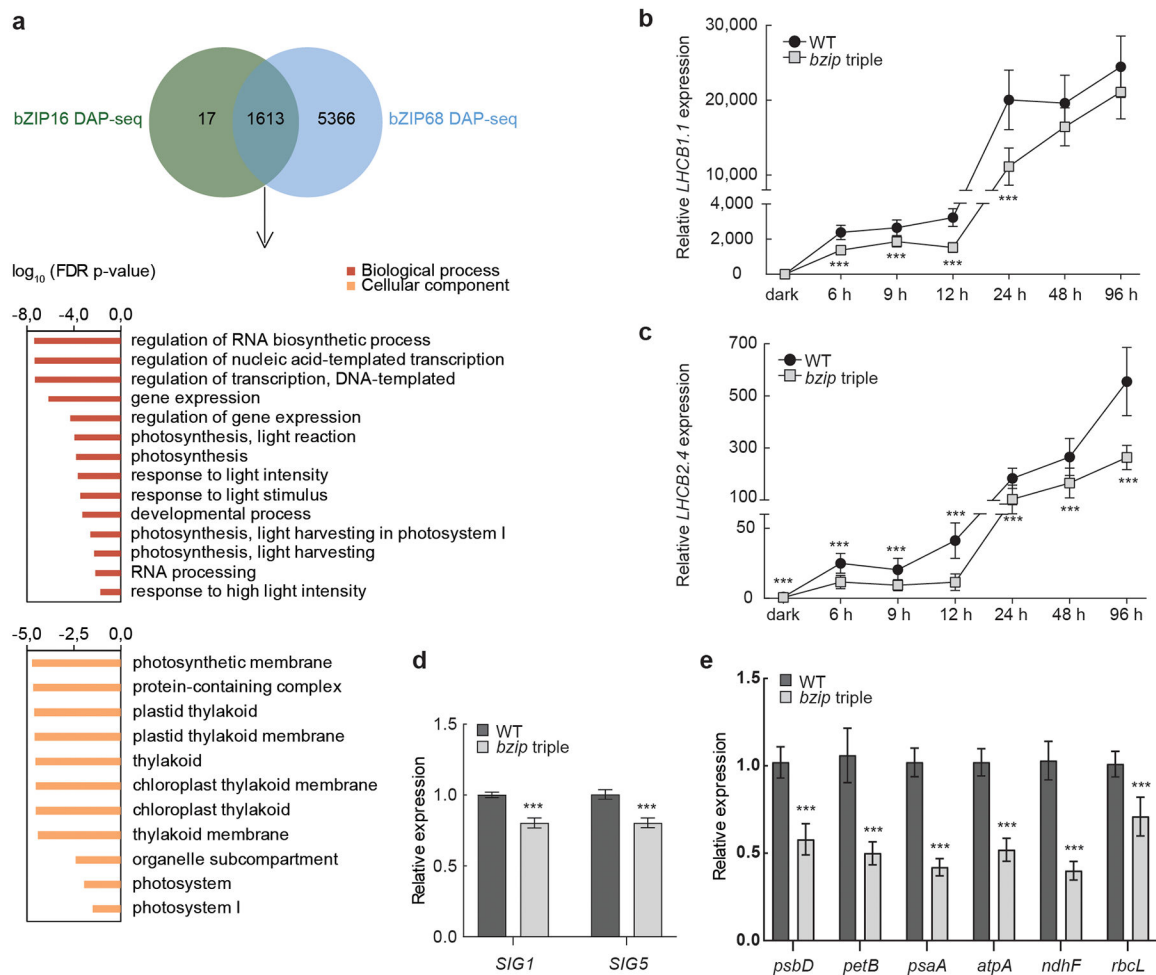


Figure 2. The bZIP proteins regulate photosynthesis-related genes in response to light.

(a) Venn diagram of identified targets and overlapping genes between bZIP16 and bZIP68 using published DAP-seq. data from Arabidopsis (O'Malley et al., 2016). GO enrichment terms are shown for the overlapping gene set. The corresponding FDR adjusted p values are indicated as horizontal bars to the left. (b-e) Etiolated seedlings of Arabidopsis WT and *bzip* triple mutant were transferred to continuous white light and analyzed for (b) *LHCBI.1* and (c) *LHCBI.4* expression normalized to Ubiquitin like protein and related to the amount present in WT in dark. Each data point represents the mean (\pm SD) of at least 3 biological replicates. (d) Seedlings exposed to 24 h of light were analyzed for *SIG1* and *SIG5* expression normalized to *PP2A* and related to the amount present in WT. Each data point represents the mean (\pm SE) of at least 3 biological replicates. (e) Seedlings exposed to 24 h of light were analyzed for the plastid genes *psbD*, *petB*, *psaA*, *atpA*, *ndhF* and *rbcL* expression normalized to *PP2A* and related to the amount present in WT. Each data point represents the mean (\pm SE) of at least 3 biological replicates. The expression of *LHCBI.1*, *LHCBI.4*, *SIG1*, *SIG5* and the plastid genes was significantly lower in the *bzip* triple mutant compared to WT as demonstrated by Student t-test: *** p < 0.001.

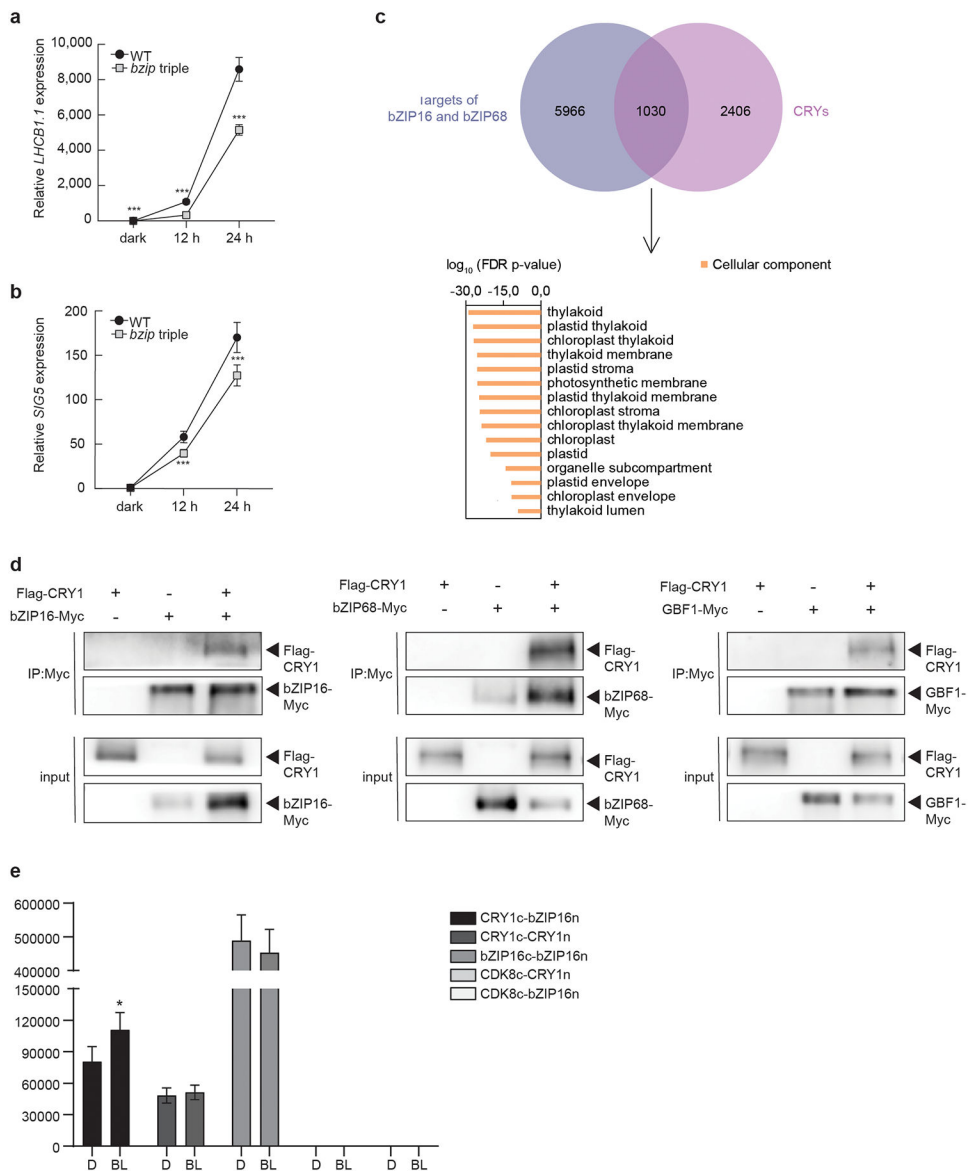


Figure 3. Cryptochromes regulate overlapping genes with the bZIP proteins and CRY1 interacts with bZIP16, bZIP68 and GFB1.

(a-b) Etiolated seedlings of Arabidopsis WT and *bzip* triple mutant were transferred to continuous blue light and analyzed for (a) *LHCBI.1* and (b) *SIG5* expression normalized to *PP2A* and related to the amount present in WT in dark. Each data point represents the mean (\pm SD) of at least 3 biological replicates. The expression of *LHCBI.1* and *SIG5* was significantly lower in the *bzip* triple mutant compared to WT as demonstrated by Student *t*-test: *** $p < 0.001$. (c) Venn diagram of identified genes and overlapping targets between bZIP16/68 and CRY1/2 using published DAP-/RNA-seq. data from Arabidopsis (He et al., 2015; O'Malley et al., 2016). The top 15 most relevant GO terms for cellular component are shown for the overlapping set of genes. The corresponding FDR adjusted *p* values are indicated as horizontal bars to the left. (d) Interaction between CRY1 and bZIP16/bZIP68/GFB1 demonstrated by Co-immunoprecipitation (Co-IP) experiment. The

Flag-CRY1 construct was co-transformed with bZIP16-Myc, bZIP68-Myc or GBF1-Myc into *N. Benthamiana* leaves and analyzed for IP using Myc-tagged magnetic beads. As a negative control, bZIP16-Myc, bZIP68-Myc and GBF1-Myc were transformed on their own. Co-IP interactions were identified between CRY1 and all three bZIP proteins by detection with an anti-Flag antibody. (e) BL stimulated interaction between CRY1 and bZIP16 demonstrated by split LUC assay. The split LUC constructs were co-transformed into *N. Benthamiana* leaves and sampled 3 days post infiltration. After 5h of incubation in dark, or 5h in dark (D) followed by 10 min exposure to blue light (BL), luciferin was added, and interaction analysed by measuring luminescence using a luminometer. As negative controls, CDK8c was co-transformed with CRY1n or bZIP16n. Interaction by reassembled luciferase was identified between CRY1c-bZIP16n, CRY1c-CRY1n and bZIP16c-bZIP16n. Each data point represents the mean (\pm SEM) of at least 4 biological replicates. Luminescence signal was significantly higher in CRY1c-bZIP16n exposed to BL compared to dark as demonstrated by Student t-test: * $p < 0.05$.

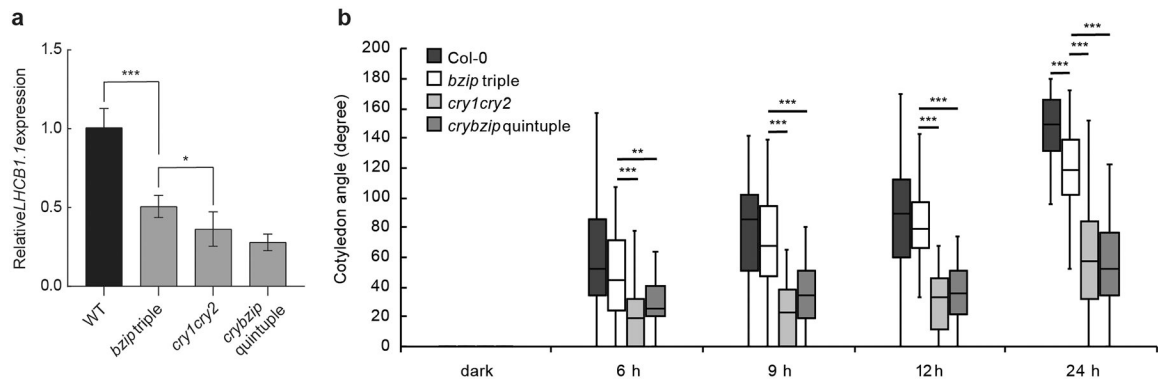


Figure 4. CRYs and the bZIPs genetically interact.

(a) Etiolated seedlings of Arabidopsis WT, *bzip* triple, *cry1cry2* and *crybzip* quintuple were transferred to continuous blue light for 24 h and analyzed for *LHCBI.1* expression normalized to *PP2A* and related to the amount present in WT. Each data point represents the mean (\pm SD) of at least 3 biological replicates. The expression was significantly lower in *bzip* triple compared to WT, and in *cry1cry2* compared to *bzip* triple, as demonstrated by Student *t*-test: *** $p < 0.001$, * $p < 0.05$. **(b)** Etiolated seedlings of Arabidopsis WT, *bzip* triple, *cry1cry2*, and *crybzip* quintuple mutant were exposed to white light and scanned to measure the cotyledon opening. Each data point represents the mean (\pm SD) of at least 25 seedlings.

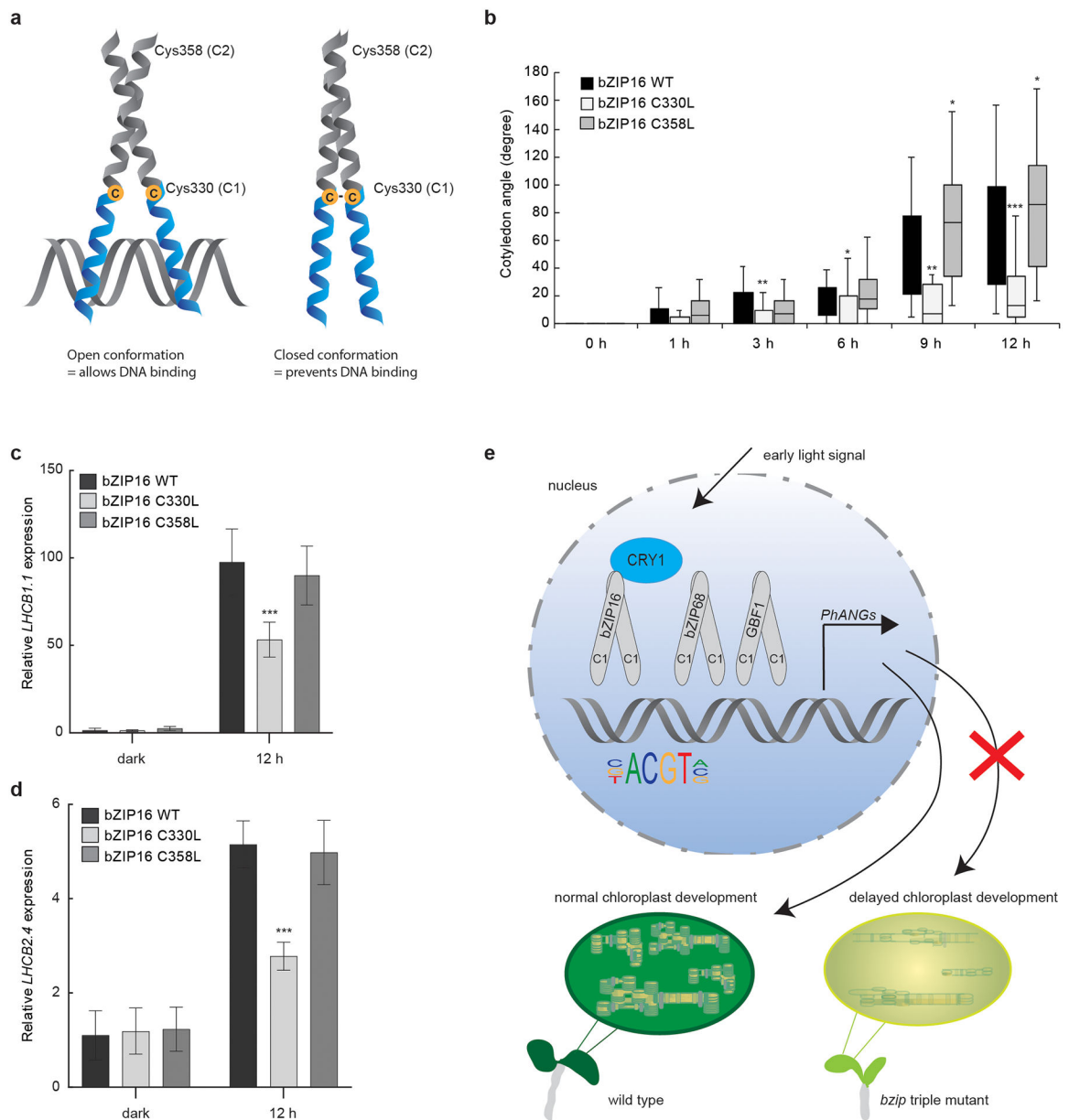


Figure 5. Activity of bZIP16 is mediated via Cys330.

(a) Illustration of the bZIP16 dimer and approximate location of the Cys330 (C1) and Cys358 (C2) residues. The two monomers interact through hydrophobic residues in the leucine zipper (colored in grey) to form a dimer and binds DNA via the basic region (colored in blue). An open conformation of the basic region allows DNA binding, while a closed formation, in which a disulfide bond is formed between the two Cys330 residues, prevents DNA binding. (b) Cotyledon opening of bZIP16WT, bZIP16C330L and bZIP16C358L overexpressing lines in Arabidopsis *bzip* triple mutant background. Etiolated seedlings were exposed to white light and scanned at the indicated time points. The cotyledon angle was measured for at least 40 seedlings per genotype and time point. The asterisks indicate significant difference between bZIP16WT and bZIP16C330L/ bZIP16C358L as

demonstrated by Student *t*-test: * $p < 0.05$, ** $p < 0.01$. **(c and d)** Etiolated seedlings of bZIP16WT, bZIP16C330L and bZIP16C358L overexpressing lines in Arabidopsis *bzip* triple mutant background were sampled in dark and following 12 h white light exposure. The samples were analyzed for **(c)** *LHCB1.1* and **(d)** *LHCB2.4* expression normalized to *PP2A* and related to the amount present in bZIP16WT in dark. Each data point represents the mean (\pm SD) of at least 3 biological replicates. The expression in 12 h was significantly different in the bZIP16C330L compared to bZIP16WT and bZIP16C358L overexpressing lines as demonstrated by Student *t*-test: * $p < 0.05$; ** $p < 0.01$. **(e)** Working model of bZIP16, bZIP68 and GBF1 function during early light signaling. Following exposure to light, the bZIP transcription factors are activated, possibly through the interaction with CRY1. The bZIPs bind DNA through the G-box *cis*-element and the combined activity of the bZIPs activates expression of *PhANGs*. The activation of these genes provides the initial signals to promote the onset of chloroplast development and photomorphogenic growth. The absence of the bZIP proteins in the *bzip* triple mutant causes down regulated nuclear transcription and loss of the anterograde signal which in turn results in a delayed chloroplast development.